the discrete Potts model,[7] and the renormalization-group[12,13] and experimental work reported here. Could there be a difference between the continuous and discrete Potts models? Some series work on the continuous model would be very interesting.

One of us (A.A.) would like to acknowledge the hospitality of the IBM Zurich Research Laboratory, where he was visiting while most of this work was done.

---

*Permanent address.

[1]K. A. Müller, W. Berlinger, and J. C. Slonczewski, Phys. Rev. Lett. 25, 734 (1970).

[2]J. C. Slonczewski, Phys. Rev. B 2, 4646 (1970).

[3]A. Aharony and A. D. Bruce, Phys. Rev. Lett. 33, 427 (1974); K. A. Müller and W. Berlinger, Phys. Rev. Lett. 35, 1547 (1975).

[4]A. D. Bruce and A. Aharony, Phys. Rev. B 11, 478 (1975).

[5]M. E. Fisher and D. R. Nelson, Phys. Rev. Lett. 32, 1350 (1974).

[6]D. Mukamel, M. E. Fisher, and E. Domany, Phys. Rev. Lett. 37, 565 (1976). Ref. 12 of this paper includes references to earlier theoretical work suggesting additional realization of the Potts model.

[7]R. B. Potts, Proc. Cambridge Philos. Soc. 48, 106 (1952).

[8]J. P. Straley and M. E. Fisher, J. Phys. A 6, 1310 (1973).

[9]R. J. Baxter, J. Phys. C 6, L445 (1973).

[10]R. V. Dítzian and J. Oitmaa, J. Phys. A 7, L61 (1974).

[11]J. P. Straley, J. Phys. A 7, 2173 (1974).

[12]G. R. Golner, Phys. Rev. B 8, 3419 (1973).

[13]J. Rudnick, J. Phys. A 8, 1125 (1975).

[14]See, e.g., J. M. Kosterlitz, D. R. Nelson, and M. E. Fisher, Phys. Rev. B 13, 412 (1976).

[15]A. D. Bruce and R. A. Cowley, J. Phys. C 6, 2422 (1973).

Electron–Surface-Plasmon Scattering Using a Parabolic Nontouching Trajectory

J. Lecante and Y. Ballu

Section d'Etudes des Interactions Gaz–Solides, Service de Physique Atomique, Centre d'Etudes
Nucléaires de Saclay, 91190 Gif-sur-Yvette, France

and

D. M. Newns

Department of Mathematics, Imperial College, London S.W.7., England

Incident electrons follow a parabolic trajectory when an electric field is applied normal to the surface of a metal crystal with force vector directed outwards. Under appropriate conditions touching trajectories may be neglected, and electron–surface-plasmon scattering is dominated by trajectories with closest approach distance. Experimental results are presented for Mo indicating that only the 1.3-eV molybdenum surface plasmon is excited. Application of this new technique to measurements such as surface-plasmon dispersion is outlined.

In this paper we report on results interpreted as inelastic scattering of an electron, traveling just outside a clean metal surface, from surface-electron excitations. By applying an electric field normal to the surface, so as to give a force F on the electron directed outwards from the surface, the electron follows an approximately parabolic orbit (Fig. 1). It is thereby demonstrated explicitly that the electrostatic potential of the surface excitations (loosely referred to below as surface plasmons) does indeed penetrate into the vacuum: The theoretical result is that the surface-plasmon potential is proportional to $\exp(-Qz)$,[1] where Q is wave vector of the excitation parallel to the surface, and z is distance measured normally outward from the surface. We believe this to be the first recognized observation of this type, though

an observation of an unresolved energy loss for electrons passing through holes in graphite[2] might bear a similar interpretation.
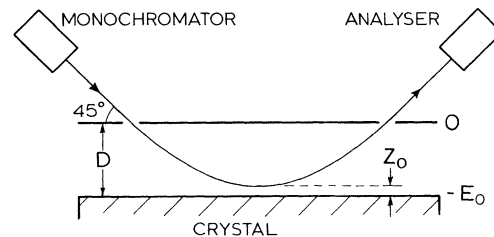

FIG. 1. One of the two experimental arrangements. Beam of energy $2E_0$ enters and leaves condenser via apertures at an incidence of approximately 45°. D is the plate separation, z_0 is the closest approach distance, and E_0 is the potential between plates.

Development of this very "clean" inelastic-scattering experiment should facilitate deeper investigation of the surface-excitation problem. This involves three main areas: (i) The image force seen by a moving external charged particle, which plays an important role in the parabolic-orbit experiment. (ii) The separation of the surface-loss spectrum, to which alone the method is sensitive, from the bulk losses in materials with complex loss spectra such as transition metals. This separation seems at present approximately possible using grazing-incidence reflection of electrons.[3] Such directly measured surface-loss spectra are complementary to calculations from reflectivity data.[4] (iii) The measurement of surface-plasmon dispersion for well-defined surfaces, which seems to present a difficult problem in the interesting region of plasmon wave vectors from $Q \sim k_F$ down to the beginning of the retardation region. The present type of experiment measures energy loss at a fairly well defined Q and might help to resolve this problem.

The probability for electron energy loss in the case of a parabolic trajectory has been calculated both semiclassically[5] and in the quantum Born approximation.[6] Semiclassically, the probability $dP(\omega)$ of energy loss between ω and $\omega + d\omega$ by an electron of velocity v parallel to the surface and closest approach distance z_0 is given by

$$dP(\omega)/d\omega = [2/(z_0 F)^{1/2}] \exp(-2z_0 \omega/v) g(\omega). \quad (1)$$

Here and in the following atomic units are used. In the classical approximation the surface-loss function is given by

$$g(\omega) = \omega^{-1} \operatorname{Im}[1 + \epsilon(\omega)]^{-1}, \quad (2)$$

where $\epsilon(\omega)$ is the solid dielectric function. The surface-plasmon wave vector excited is $Q_\omega \simeq \omega/v$ and the exponential factor comes from evaluating the square of the surface-plasmon field $\exp(-Q_\omega z)$ at z_0, most of the scattering taking place near this turning point. The exponential factor can be said to attenuate the scattering probability unacceptably for $z_0 \gtrsim 3Q_\omega^{-1}$.

The constant outward force on the electron due to the external electric field is modified by the image force. Corrections to the classical image force due to motion of the charged particle parallel to the surface have been calculated by various authors.[7] In particular, the numerical evaluation by Muscat[7] shows that in the present problem the classical image force can be used to good accura-

cy. The potential seen by the electron then is

$$V(z) = -Fz - 1/4z. \quad (3)$$

The maximum in (3) at $z_m = \frac{1}{2}F^{1/2}$ limits nontouching trajectories to $z_0 > z_m$; we shall for simplicity assume that the constant-force theory can be used provided z_0 lies in the nontouching region.

It is also required that the electron wavelength and recoil effects not be too large. At z_0 the electron wave vector normal to the surface[6] is $\alpha = (2F)^{1/3}$ and this must considerably exceed z_0^{-1}. Recoil effects displace the turning point of the final-state parabolic trajectory to z_f, whose mean value is $\bar{z}_f$. We require that the quantities z_1 and z_2, given by

$$z_1 = \bar{z}_f - z_m = Q_\omega^2/2F, \quad (4)$$

$$z_2^2 = \langle (z_f - \bar{z}_f)^2 \rangle_{\text{mean}} = Q_\omega/2F \quad (5)$$

be small compared with z_0.

Planning the experiment requires primarily that, at the point $z_0 = z_m$ of maximum attainable scattering probability, the exponent $2Q_\omega z_m$ in (1) not be too large to ensure reasonable scattering probability. This, together with small recoil effects, can be ensured provided that F is large and ω small. The quantum uncertainty α^{-1} must not, however, become excessive. The situation is illustrated in Table I for the geometry of Fig. 1, with an F value approaching the maximum attainable in the present apparatus. The quantity P in Table I is the probability integrated over energy for a single surface excitation of frequency ω_s, in which case $g(\omega) = \pi\delta(\omega - \omega_s)/4$. It is seen from Table I that we are limited by the exponential attenuation to excitations having energies of little more than an electron volt, but in this region the other conditions imposed are reasonably well satisfied.

The apparatus, located in an ultrahigh-vacuum

TABLE I. Scattering data at $z_0 = z_m$.

E_0[a] (eV)	$\hbar\omega_s$[b] (eV)	P[c]	z_m (Å)	α^{-1} (Å)	z_1 (Å)	z_2 (Å)	λ (Å)
2000	1	10	138	27	−0.7	11	910
2000	3	0.4	138	27	−6	19	13
2000	10	7×10^{-6}	138	27	−66	34	3×10^{-3}

[a]Electron beam of energy $2E_0$ entering condenser at 45° incidence.
[b]Single surface excitation of frequency ω_s.
[c]Calculated for a condenser plate separation of $D = 2 \times 10^7$ a.u.

chamber, consists of a fixed electron monochro-
mator and an energy analyzer rotatable about a
vertical axis. Both units are basically hemispher-
ical analyzers equipped with entrance and exit op-
tics; for a detailed description the reader is re-
ferred elsewhere.[8] At a current of 10^{-10} A the
analyzer typically records a peak of 20 meV full
width at half-maximum superimposed on a blank
background. The target cell, also rotatable about
a vertical axis, contains a Mo single crystal
whose (001) surface is at a distance of 1 mm from
a parallel insulated Mo plate. The latter in some
experiments contains parallel slits 4 mm apart
for the electron beam as in Fig. 1, while in others
it is unperforated and the beam is led in and out
through the ends of the condenser. The manipula-
tor allows small adjustments of the Mo crystal
along the (001) direction. The cell is surrounded
by a cylindrical Mo grid perforated in front of
the monochromator.

The Mo surface is cleaned by oxidation in 10^{-6}
Torr of oxygen at 1000°C for 4 h, followed by an-
nealing at 1600°C. Clean surfaces can be re-
stored after adsorptions by flashes at 1600°C in
vacuum. Surface cleanliness during CO or O_2 ad-
sorption is followed by means of work-function
change, this being compared with that in a paral-
lel low-energy-electron-diffraction–Auger exper-
iment.

The width of the electron beam in this appara-
tus greatly exceeds z_m, giving rise to a range of
trajectories characterized by their z_0 values.
We can distinguish three categories of electron,
those with $z_0 \gg z_m$, with $z_0 \gtrsim z_m$, and with $z_0 < z_m$.
The first group should contribute only to the elas-
tic peak, while the second undergoes inelastic
scattering according to the above discussion.
The third group which strike the surface do so at
a finite grazing angle $\beta = (\pi/2 - \text{angle of incidence})$.
For the conditions of Table I $\beta \gtrsim 1°$. Now the co-
efficient of specular elastic reflection for near
grazing electrons in the 10^3-eV energy range is
observed in this apparatus to be less than 10^{-4} on
Mo (001) surfaces, and the angular discrimina-
tion of the analyzer seen from the cell center is
of order 10^{-3} rad. Taking these two factors to-
gether, and ignoring lens effects at entrance and
exit to the condenser, an effective one-dimension-
al "cross section"[9] of $\lambda < 2$ Å is obtained for spec-
ular *elastic* electrons entering the analyzer [we
here use Eq. (28) of Ref. 6]. This result is rela-
tively low.

We therefore argue that, with appropriate ad-
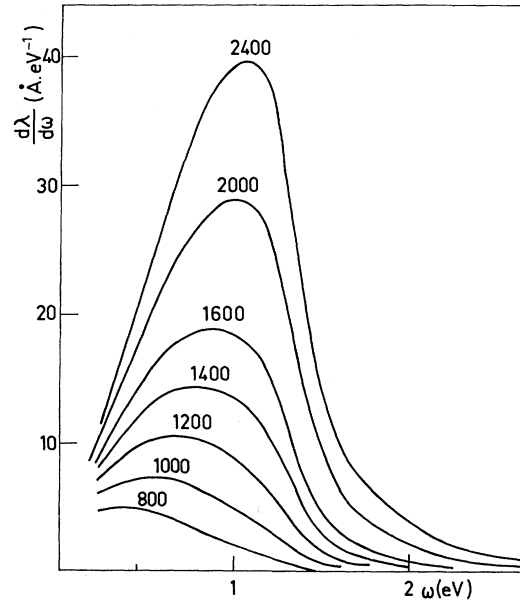justment, mostly inelastic electrons from the

FIG. 2. Theoretical differential linear cross section
for Mo target in configuration of Fig. 1, using Eq. (6)
with $D = 1$ mm. Curves labeled by E_0 values in volts.

second group $(z_0 > z_m)$ can be observed in the ana-
lyzer. Assuming that all $z_0 > z_m$ are equally prob-
able, we integrate the semiclassical linear-poten-
tial formula (1) over the range $z_m < z_0 < \infty$. For
the configuration of Fig. 1 the approximate result
is

$$\frac{d\lambda}{d\omega} = \left(\frac{2D}{z_m}\right)^{1/2} \exp\left[-\frac{\omega}{E_0}\left(\frac{D}{2}\right)^{1/2}\right]\frac{g(\omega)}{\omega}, \quad (6)$$

where D is the plate separation. Results calculat-
ed from Eq. (6) are shown in Table I for the sin-
gle-excitation model, with λ the linear cross sec-
tion integrated over energy. In Fig. 2 we plot
theoretical curves for Mo at various voltages E_0,
using in (2) the dielectric function determined
from optical reflection data.[4] The Mo results
show only a single hump dominated by the surface
plasmon of Mo at 1.3 eV to which we have previ-
ously drawn attention.[3] This feature is seen to
entirely dominate the spectrum in Fig. 2, the sur-
face plasmons at higher ω being strongly attenu-
ated by the exponential factor in (6). It is also
noticed that, because the 1.3-eV surface plasmon
is only a small contribution to the total loss func-
tion (2) of Mo, λ for the single-excitation model
at $\omega_s = 1$ eV in Table I is much greater than the
area under the curves in Fig. 2.

In Fig. 3 we show experimental results for the
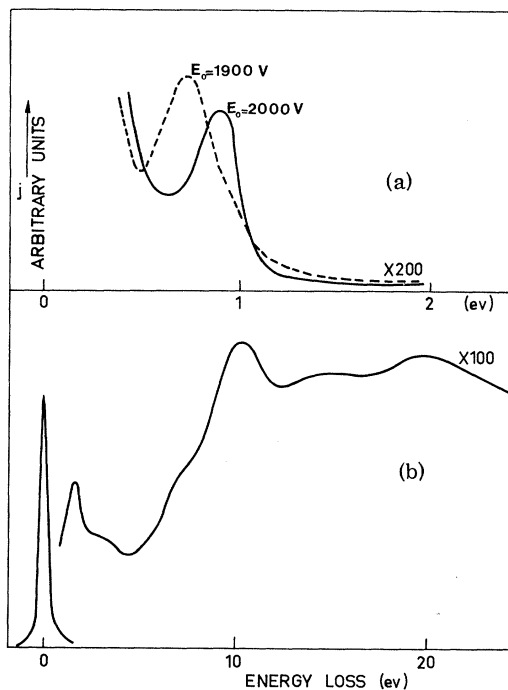configuration of Fig. 1. It is possible by gradual-

FIG. 3. Experimental results for current j in analyz-
er (arbitrary units) as a function of energy loss ω.
(a) Touching trajectory; (b) parabolic trajectory.
Curves labeled by E_0 values in volts.

ly increasing the voltage between the condensor
plates to pass successively from energy-loss
spectra of the type shown in Fig. 3(b), and finally
to a spectrum showing only the elastic peak. The
spectrum shown in Fig. 3(a) is characteristic of
an electron beam *reflected* at a grazing incidence,
with or without a normal electric field, as dis-
cussed in Ref. 3. The exponential factor charac-
teristic of the parabolic experiment is then lack-
ing and the loss spectrum is proportional to $g(\omega)$
of Eq. (2), showing the surface plasmons at 1.3,
10, and 20 eV. On the other hand, the curves of
Fig. 3(b) resemble those of Fig. 2 in having a
hump at $\omega \sim 1$ eV and an absolutely clean back-
ground for $\omega \gtrsim 3$ eV. The peak is attributed to the
Mo (100) surface in that its sensitivity to contami-
nation—disappearance after 1 night at 10^{-8} Torr
of residual gases—is similar to the 1.3-eV peak
in Fig. 3(a), with restoration after a flash at
1600°C. It is so characteristic of the parabolic
scattering experiment as to fairly convincingly
uphold such an interpretation. However a feature
of the calculated curves in Fig. 2 which we have
not been able to confirm experimentally is the
shift in peak position as a function of E_0. The
correlation between peak position and E_0 is found

to be not very reproducible in the range 800 eV
$< E_0 < 2000$ eV within which the phenomenon is ob-
servable. An extreme example is shown in Fig.
3(b) (broken curve) where a peak at 0.75 eV oc-
curs at an E_0 value only slightly less than that
giving a peak displaced to 0.95 eV (full curve).
We attribute this to local variations in electric
field F giving rise to corresponding variations in
z_m and thus in the strongly varying exponential
factor $\exp(-2z_m\omega/V)$ in (6). Although our method
of cleaning leads to samples having a well-defined
low-energy-electron-diffraction pattern, they are
not expected to be macroscopically flat. Since
the present experiment theoretically demands
that the surface be flat within a fraction of 130 Å
over a horizontal distance of order 10^5 Å, the in-
tervention in practice of macroscopic irregulari-
ties leading to field inhomogeneities perhaps is
not surprising.

In conclusion, two problems need to be sur-
mounted before the program introduced at the be-
ginning of this article can be fully realized. The
surface-flatness problem is not believed to be in-
surmountable. A well-known case of a surface
both macroscopically and microscopically flat
does, for example, exist in the field emission
tip, and in fact the use of this has been discussed
in Ref. 6. The strong exponential attenuation
characteristic of Eq. (6), whose positive side is
of course the fixing of the surface-plasmon wave
vector, may be overcome by using sufficiently
strong fields and high electron energies. Further
work in the direction of overcoming these obsta-
cles is continuing.

[1]R. H. Ritchie, Phys. Rev. 106, 874 (1957); E. A.
Stern and R. A. Ferrell, Phys. Rev. 120, 130 (1960);
A. A. Lucas and M. Sunjic, Phys. Lett. 38A, 413 (1972).
[2]M. Isaacson, J. P. Langmore, and H. Rose, Optik
(Stuttgart) 41, 92 (1974).
[3]Y. Ballu, J. Lecante, and D. M. Newns, Phys. Lett.
57A, 159 (1976).
[4]J. H. Weaver, D. W. Lynch, and C. G. Olson, Phys.
Rev. B 10, 501 (1974).
[5]J. P. Muscat, Solid State Commun. 18, 1089 (1976).
[6]B. Gumhalter and D. M. Newns, Surf. Sci. 50, 465
(1975).
[7]N. Takimoto, Phys. Rev. 146, 366 (1966); J. Harris
and R. O. Jones, J. Phys. C 7, 3751 (1974); J. P. Mus-
cat, unpublished.

[8]Y. Ballu and J. Lecante, to be published.

[9]For an incident electron beam traveling parallel to the surface, of current J per unit length normal to sur- face, the total current scattered into a particular channel is $J\lambda$, where λ is the linear cross section for the channel.

Laser-Modulated Photoemission in Semiconductors

M. Wautelet and L. D. Laude
Faculté des Sciences, Université de l'Etat, Mons, Belgium
(Received 12 July 1976)

A novel, double-beam photoemission experiment is described in which electron energy distributions are obtained from semiconductors by modulating the ultraviolet photocurrent with a tunable, flash-excited, dye-laser beam. Double-beam photoemission spectra are demonstrated, in the case of tellurium, to result from optical transitions alone within the unperturbed bulk band structure of the solid. Unique information is obtained on the conduction-band-states distribution below vacuum level, within which a forbidden gap is demonstrated to exist between 2.5 and 4.7 eV above valence-band edge.

Information on the band structure of a solid is currently obtained from the interaction of a *single* electromagnetic beam with the solid.[1] However, this information may be shadowed by structural peculiarities resulting in uncertainties in the interpretation of the optical spectra. A more powerful way to investigate the electronic structure of a solid would be to associate two different optical-absorption processes initiated in the solid by two independent optical sources and to obtain an experimental evidence for such a coupling. The object of this Letter is to report on the results of an experimental inquiry which provides such an evidence and to demonstrate the advantage of the technique in terms of band structure.

The experiment uses basically a photoemission setup[2] in which a continuous uv beam and a pulsed, coherent beam are focused at 45° incidence onto the same ultrahigh-vacuum-cleaved crystal face. uv photons, of energy ϵ, initiate the excitation of valence electrons into the conduction band. These electrons are further emitted into vacuum, collected on a spherical analyzer, and contribute to the photoemission current, I. The coherent beam is provided by a Chromatix CMX-4 flash-excited dye laser in the 2–4-eV range. Pulses are delivered at adjustable frequencies, Ω_L, between 5 and 25 Hz. The total diameter of the beam is approximately 4 mm. The pulse power is 6 and 0.4 kW, corresponding to photon fluxes of 10^{16} and 3×10^{14} photons per pulse, at $h\nu_L = 2.08$ and 4.16 eV, respectively. Should a coupling take place within the solid between the uv photoemission process and the laser beam, an ac contribution to I would be produced at Ω_L. To obtain a detectable $I(\Omega_L)$ would require a laser beam such that the proportion between absorbed laser photons

and valence electrons behind the solid surface over a depth equal to l_e, the electron mean free path, be of the order of, at least, a few percent. Taking the valence-electron number to be about 10^{16} over, say, 20 Å, one sees that the laser used in this work does fulfill this mandatory condition. This ac current $I(\Omega_L)$ is selectively detected by passing I through a lockin amplifier phase-locked on Ω_L. The amplifier output is then stored in a multichannel signal analyzer. This output, namely the Ω_L derivative of $I(\Omega_L)$, represents the energy distribution curve (EDC) of *only* those emitted electrons which have "seen" both the uv and laser beams.

This double-beam photoemission (DBP) experiment, described here for the first time, has been tested on several semiconductors so far. Most impressive are the results obtained on $(10\bar{1}0)$ tellurium because of the distinct characteristics of its electronic structure. Therefore, some of the Te data will be presented in this Letter to demonstrate the unique advantages of the DBP technique. More complete Te data together with those on Ge, Si, Se, and others will be published elsewhere.

Two series of spectra have been obtained on $(10\bar{1}0)$ Te at $h\nu_L = 2.08$ and 4.16 eV in the 3.2–8.7-eV uv range. Some of these spectra are shown in Fig. 1, together with a (single-beam) EDC obtained at $\mathscr{E} = 7.71$ eV. In Fig. 1(b) at $h\nu_L = 2.08$ eV, one compares the 5.60- and 7.71-eV spectra; these have equal widths but show different profiles; in Fig. 1(c) at $h\nu_L = 4.16$ eV, the 7.71-eV spectrum is compared to the 3.51-eV one. The low-energy part of the 7.71-eV spectrum and the total 3.51-eV spectrum do compare well in width and position on the energy axis, differences ap-